HIGH-HARMONIC MM–WAVE FREQUENCY MULTIPLICATION USING A GYROCON–LIKE DEVICE*

F. Toufexis[†1], S.G. Tantawi, A. Jensen, V.A. Dolgashev,
A. Vrielink[1], M.V. Fazio, SLAC, Menlo Park, CA 94025
P. Borchard, Dymenso LLC, San Francisco, CA 94115
[1]Also at Department of Electrical Engineering, Stanford University, Stanford, CA 94305

Abstract

Traditional linear interaction RF sources, such as Klystrons and Traveling Wave Tubes, fail to produce significant power levels at millimeter wavelengths. This is because their critical dimensions are small compared to the wavelength, and the output power scales as the square of the wavelength. We present a vacuum tube technology, where the device size is inherently larger than the operating wavelength. We designed a low–voltage mm–wave source, with an output interaction circuit based on a spherical sector cavity. This device was configured as a phased-locked frequency multiplier. We report the design and cold test results of a proof-of-principle fifth harmonic frequency multiplier with an output frequency of 57.12 GHz.

INTRODUCTION

Millimeter–waves refer to the part of the frequency spectrum above 50 GHz up to 1 THz. This part of the spectrum is still unexploited because of the lack of compact mm-wave sources [1–4] – especially amplifiers – that are able to provide substantial amount of power. Compact high power mm-wave sources will enable several applications such as spectroscopy, high–resolution medical imaging, navigation through sandstorms, spectroscopic detection of explosives, high bandwidth, low probability of intercept communications, and space radars for debris tracking of objects less that 5 cm that present hazards to space assets, such as communications satellites.

Gyrotrons and gyro–amplifiers [5–9] are powerful mm-wave sources; however, they require a superconducting magnet which renders these devices very large and impractical for many applications. Incarnations of Gyrotrons that operate at higher harmonics are the Large Orbit Gyrotrons [10–13] and Gyro–multipliers [14–17]. Frequency multiplying tubes, such as Gyrocons [18–24] and Magnicons [23,25–32], are an attractive alternative to conventional vacuum amplifiers. In such tubes, a continuous electron beam is helically deflected, by exciting two orthogonal polarizations in a TM_{11} deflecting cavity. The beam arrives at the output cavity as a wave of electron current rotating around the axis of symmetry, and excites a traveling electromagnetic wave. The synchronism condition is given by $\omega_{RF} = m\omega_{LO}$, where ω_{LO} is the angular frequency of the deflecting cavity, ω_{RF} is the
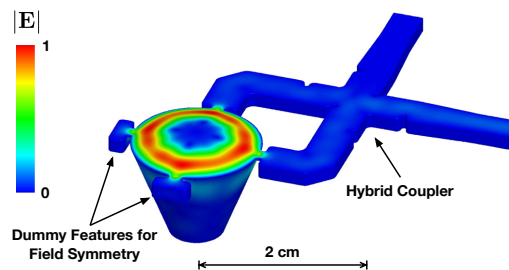
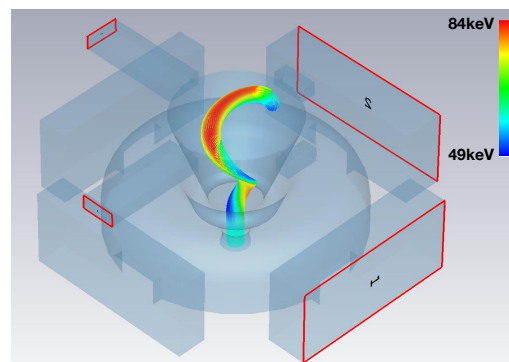Figure 1: Vacuum model and surface electric fields of the output circuit.

Figure 2: CST Particle Tracking.

angular frequency of the generated signal in the output cavity, and m is the number of azimuthal variations of the target eigenmode in the output cavity. However, to our knowledge the Gyrocons that have been experimentally demonstrated only operated with $m = 1$, and there is only a theoretical analysis for $m = 2$ [24]. The output cavities of these devices employed beam pipes shielded with aluminum foils, which required a relativistic beam. Furthermore, a complicated magnetic field profile was necessary to guide the beam through the beam pipes. Scaling Gyrocons to higher frequencies requires reducing the current dramatically, thus limiting the output power to levels already achieved with traditional devices.

We have developed a new Gyrocon–like mm–wave source, with an output interaction circuit based on a spherical sector cavity. We have designed, manufactured and hot-tested a proof–of–principle device, and in this work we report the design and cold–test data of the input and output circuits.
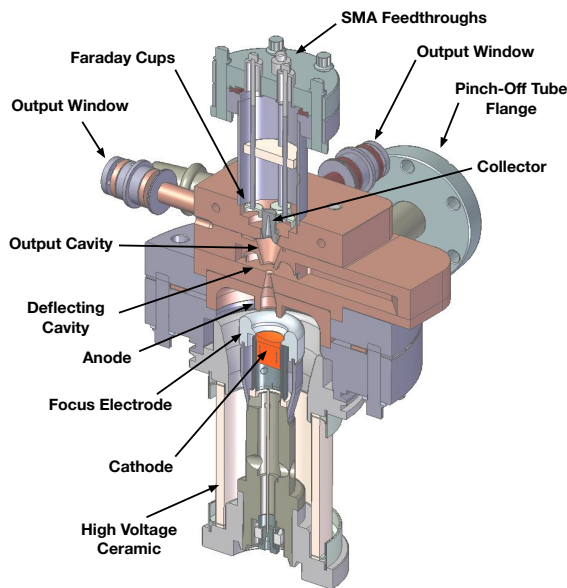
Figure 3: Device Design.

RF DESIGN

For the output cavity we used a spherical sector cavity that supports a whispering gallery TM_{nm} mode in the r–direction (in spherical coordinates), of high azimuthal variation, suitable for interaction with an electron beam also traveling in the r–direction, without any further redirection. The field profile of such modes is described in [33]. As shown in Fig. 1, the mode is well confined at the top of the resonator, allowing the bottom to be open for the electron beam to enter. This opening is larger than the wavelength, which distinguishes our approach from traditional devices having beam pipes being small fractions of the wavelength.

Combining helical beam deflection at a low frequency with the spherical sector resonator as the output cavity yields several advantages over existing solutions. As the beam travels in the r–direction, helically deflected, the effect of space charge decreases. Since the frequency context is not encoded as longitudinal bunching, space charge is not a limiting factor any more, in contrast to devices like klystrons or TWTs. We further observed, that when multiplying frequency from X–band (8–12 GHz) to V–band (50–75 GHz) or W–Band (75–110 GHz), the dimensions of the output resonator allow for a device that is small enough that beam expansion is minimal, even without any focusing, but large enough to allow for significant current to go through. There is, therefore, no need for a narrow beam pipe or any sort of magnetic focusing or beam guidance compared to Gyrocons. Further, limiting m to be an odd number allows coupling of this resonator using two orthogonally placed waveguides and a hybrid coupler that combines the two outputs of the resonator to one, as shown in Fig. 1.

We designed, manufactured and cold–tested the vacuum tube frequency multiplier shown in Fig. 3, which multiplies an input frequency of 11.424 GHz times 5, producing 57.12 GHz. The tube is designed to operate at a beam
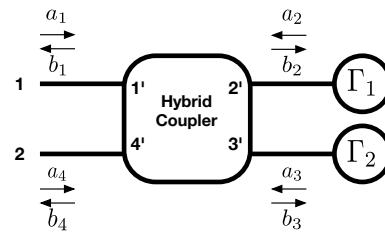

Figure 4: Equivalent circuit model of two different single–moded cavities, coupled through a hybrid coupler.

voltage of 60 kV and current of 8.8 A. Using an in–house particle tracking code, we estimated that the input power required at X–Band is in the order of 70 kW, and the expected output power at V–Band is in the order of 60 kW with a beam to RF efficiency of 12 %.

The initial design point was $m = 5$ and $n = 21$ because the radius of the cavity is approximately 2 cm, which is small enough to prevent significant expansion of the electron beam. We optimized the cone angle so that there is no parasitic mode within 500 MHz. Since the output cavity also acts as the beam collector, we added a cone made of molybdenum, so that when there is no RF in the deflecting cavity, the collector is not damaged. A biplanar hybrid coupler [34] is used to create the correct phase difference. However, this coupling scheme breaks the degeneracy of the deflecting modes. To improve the symmetry of the modal fields, we added two terminated waveguide pieces with coupling irises. The size of these waveguide pieces was chosen to prevent any resonances near the frequency of interest. Table 1 summarizes the designed and measured properties of the two degenerate eigenmodes in the output cavity.

The input deflecting cavity shape was optimized to minimize the required X–Band power, for a beam voltage of 60 kV. The input cavity coupling scheme is the same as in the output cavity. Table 2 summarizes the designed and measured properties of the two degenerate eigenmodes in the input cavity.

COLD TEST

To measure the properties of these cavities through a hybrid coupler, we developed the following model. From an equivalent circuit model of a single–moded cavity with resonant frequency f_0, the reflection coefficient as a function of frequency f, intrinsic quality factor Q_0, and coupling

Table 1: Summary of Output Cavity Parameters

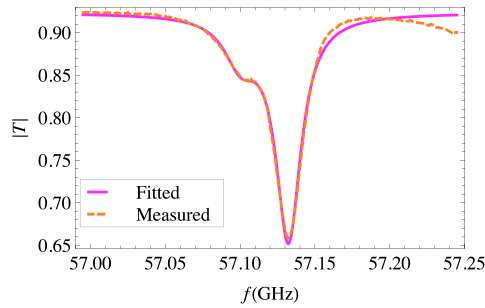|	$f_0\ (GHz)$	Q_0	β_c	Q_t
Designed #1	57.1239	7573	0.985	3814
Designed #2	57.1240	7494	0.960	3824
Measured #1	57.1000	2189	0.059	2066
Measured #2	57.1324	3592	0.399	2566

Figure 5: Output Cavity Transmission Measurement versus Fitted Model.

coefficient β_c is given by:

$$\Gamma\left(f; f_0, Q_0, \beta_c\right) = \frac{1 - jQ_0\delta\left(f; f_0\right) - \beta_c}{1 - jQ_0\delta\left(f; f_0\right) + \beta_c}, \quad (1)$$

where:

$$\delta\left(f; f_0\right) = \frac{f}{f_0} - \frac{f_0}{f}. \quad (2)$$

Our device can be modeled as shown in Fig. 4. There are two different cavities with reflection coefficients $\Gamma_1 = \Gamma\left(f; f_0^1, Q_0^1, \beta_c^1\right)$ and $\Gamma_2 = \Gamma\left(f; f_0^2, Q_0^2, \beta_c^2\right)$. The scattering matrix of the hybrid coupler is given by:

$$\mathbf{S}_{hc} = -\frac{1}{\sqrt{2}}\begin{pmatrix} 0 & j & 1 & 0 \\ j & 0 & 0 & 1 \\ 1 & 0 & 0 & j \\ 0 & 1 & j & 0 \end{pmatrix}. \quad (3)$$

Solving the equation $\mathbf{b} = \mathbf{S}_{hc}\mathbf{a}$, and noting that $a_4 = 0$, $a_2 = -b_2\Gamma_1$ and $a_3 = -b_3\Gamma_2$, we can get the reflection and transmission of the entire system as:

$$\Gamma = \frac{b_1}{a_1} = \frac{1}{2}\left(\Gamma_1 - \Gamma_2\right), \quad (4a)$$

$$T = \frac{b_4}{a_1} = -\frac{1}{2}j\left(\Gamma_1 + \Gamma_2\right). \quad (4b)$$

We can see from (4) that for identical cavities ($\Gamma_1 = \Gamma_2$), the reflection becomes zero, and the transmission becomes the same as in a single–moded cavity.

We fitted the measured S–parameters of the output cavity. The results are shown in Table 1. The coupling factor and intrinsic quality factor of the first mode deviate significantly from the designed. We suspect that braze material went inside the coupling irises, thus reducing the coupling especially for the first mode. Next, we fitted the measured

Table 2: Summary of Input Cavity Parameters

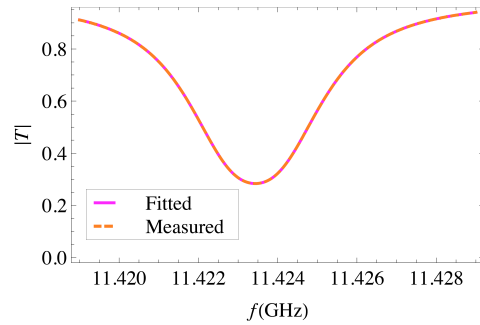|	f_0 (GHz)	Q_0	β_c	Q_t
Designed #1	11.4252	5821	1.013	2891
Designed #2	11.4257	5829	1.018	2888
Measured #1	11.4225	5903	0.832	3221
Measured #2	11.4244	5899	0.843	3200

Figure 6: Deflecting Cavity Transmission Measurement versus Fitted Model.

S–parameters of the input deflecting cavity. The results are shown in Table 2. The frequencies, coupling factor, and quality factor are very close to the designed; however, there is a significant frequency deviation between the two degenerate eigenmodes, on the order of f_0/Q_0. The measured transmission and fit are shown in Fig. 6.

SUMMARY

We designed, built and hot–tested a low–voltage mm–wave source, with an output interaction circuit based on a spherical sector cavity. This device was configured as a fifth harmonic phased-locked frequency multiplier with an output frequency of 57.12 GHz. We presented the design and cold test results. Hot test results will be reported in future publications.

ACKNOWLEDGMENTS

REFERENCES

[1] V. L. Granatstein, R. K. Parker, and C. M. Armstrong, "Vacuum electronics at the dawn of the twenty-first century," *Proceedings of the IEEE*, vol. 87, no. 5, pp. 702–716, May 1999.

[2] P. H. Siegel, "Terahertz technology," *IEEE Transactions on Microwave Theory and Techniques*, vol. 50, no. 3, pp. 910–928, Mar 2002.

[3] J. H. Booske, R. J. Dobbs, C. D. Joye, C. L. Kory, G. R. Neil, G. S. Park, J. Park, and R. J. Temkin, "Vacuum electronic high power terahertz sources," *IEEE Transactions on Terahertz Science and Technology*, vol. 1, no. 1, pp. 54–75, Sept 2011.

[4] S. Armstrong, "The truth about thz," *IEEE Spectrum*, Sept 2012.

[5] E. A. Nanni, S. M. Lewis, M. A. Shapiro, R. G. Griffin, and R. J. Temkin, "Photonic-band-gap traveling-wave gyrotron amplifier," *Phys. Rev. Lett.*, vol. 111, p. 235101, Dec 2013.

[6] M. Y. Glyavin, A. G. Luchinin, and G. Y. Golubiatnikov, "Generation of 1.5-kw, 1-thz coherent radiation from a gyrotron with a pulsed magnetic field," *Phys. Rev. Lett.*, vol. 100, p. 015101, Jan 2008.

[7] K. L. Felch, B. G. Danly, H. R. Jory, K. E. Kreischer, W. Lawson, B. Levush, and R. J. Temkin, "Characteristics and applications of fast-wave gyrodevices," *Proceedings of the IEEE*, vol. 87, no. 5, pp. 752–781, May 1999.

[8] K. R. Chu, "The electron cyclotron maser," *Rev. Mod. Phys.*, vol. 76, pp. 489–540, May 2004.

[9] T. Notake, T. Saito, Y. Tatematsu, A. Fujii, S. Ogasawara, L. Agusu, I. Ogawa, T. Idehara, and V. N. Manuilov, "Development of a novel high power sub-thz second harmonic gyrotron," *Phys. Rev. Lett.*, vol. 103, p. 225002, Nov 2009.

[10] S. Sabchevski, T. Idehara, M. Glyavin, S. Mitsudo, I. Ogawa, K. Ohashi, and H. Kobayashi, "Design of a large orbit gyrotron with a permanent magnet system," *Vacuum*, vol. 62, no. 2–3, pp. 133 – 142, 2001.

[11] V. L. Bratman, Y. K. Kalynov, and V. N. Manuilov, "Large-orbit subterahertz and terahertz gyrotrons," *Radiophysics and Quantum Electronics*, vol. 52, no. 7, pp. 472–481, 2009.

[12] V. L. Bratman, and Yu. K. Kalynov, and V. N. Manuilov, "Large-orbit gyrotron operation in the terahertz frequency range," *Phys. Rev. Lett.*, vol. 102, p. 245101, Jun 2009.

[13] X. Li, J. Lang, Y. Alfadhl, and X. Chen, "Study of an eighth-harmonic large-orbit gyrotron in the terahertz band," *IEEE Transactions on Plasma Science*, vol. 43, no. 2, pp. 506–514, Feb 2015.

[14] I. V. Bandurkin and A. V. Savilov, "Suppressing electron bunching at low harmonics in gyromultipliers of the klystron type," *Technical Physics Letters*, vol. 33, no. 9, pp. 795–798, September 2007.

[15] I. V. Bandurkin, V. L. Bratman, A. V. Savilov, S. V. Samsonov, and A. B. Volkov, "Experimental study of a fourth-harmonic gyromultiplier," *Physics of Plasmas*, vol. 16, no. 7, 2009.

[16] I. V. Bandurkin and S. V. Mishakin, "Gyromultiplier with sectioned cavity," *Physics of Plasmas*, vol. 17, no. 11, 2010.

[17] D. A. Constable, I. V. Bandurkin, W. He, A. W. Cross, A. V. Savilov, A. D. R. Phelps, V. L. Bratman, and K. Ronald, "Numerical investigation of gyro-multiplier schemes," in *Vacuum Electronics Conference (IVEC), 2012 IEEE Thirteenth International*, April 2012, pp. 529–530.

[18] G. I. Budker, M. M. Karliner, I. G. Makarov, S. N. Morozov, O. A. Nezhevenko, G. N. Ostreiko, and I. A. Shekhtman, "The gyrocon, a highly efficient converter of energy from powerful relativistic beams for microwave supplies in charged-particle accelerators," *Soviet Atomic Energy*, May.

[19] G. I. Budker, and M. M. Karliner, and I. G. Makarov, and S. N. Morozov, and O. A. Nezhevenko, and G. N. Ostreiko, and I. A. Shekhtman, "The Gyrocon: An Efficient Relativistic High Power Vhf generator," *Part. Accel.*, vol. 10, pp. 41–59, 1979. [Online]. Available: http://cds.cern.ch/record/1107968

[20] P. J. Tallerico and J. E. Rankin, "The gyrocon: A high-efficiency, high-power microwave amplifier," *IEEE Transactions on Electron Devices*, vol. 26, no. 10, pp. 1559–1566, Oct 1979.

[21] P. J. Tallerico, "Status of the los alamos gyrocon," *IEEE Transactions on Nuclear Science*, vol. 28, no. 3, pp. 2797–2799, June 1981.

[22] P. J. Tallerico, "A 150-kw, 450-mhz gyrocon rf generator," *IEEE Transactions on Nuclear Science*, vol. 30, no. 4, pp. 3420–3422, Aug 1983.

[23] A. Nezhevenko, "Gyrocons and magnicons: microwave generators with circular deflection of the electron beam," *IEEE Transactions on Plasma Science*, vol. 22, no. 5, pp. 756–772, Oct 1994.

[24] V. V. Matveenko and A. K. Sinitsyn, "Multiplication of frequency in a gyrocon with a longitudinal magnetic field," in *Vacuum Electronics Conference (IVEC), 2011 IEEE International*, Feb 2011, pp. 449–450.

[25] M. Karliner, E. Kozyrev, I. Makarov, O. Nezhevenko, G. Ostreiko, B. Persov, and G. Serdobintsev, "The magnicon — an advanced version of the gyrocon," *Nuclear Instruments and Methods in Physics Research Section A: Accelerators, Spectrometers, Detectors and Associated Equipment*, vol. 269, no. 3, pp. 459 – 473, 1988.

[26] V. E. Akimov, Y. V. Baryshev, B. S. Estrin, M. M. Karliner, I. V. Kazarezov, E. Kozyrev, G. I. Kuznetsov, I. G. Makarov, O. A. Nezhevenko, G. N. Ostreiko, B. E. Persov, G. V. Serdobintsev, M. A. Tiunov, V. P. Yakovlev, and I. A. Zapryagaev, "High power X band pulse magnicon," *Conf. Proc.*, vol. C900612, pp. 1000–1002, 1990.

[27] W. M. Manheimer, "Theory and conceptual design of a high-power highly efficient magnicon at 10 and 20 ghz," *IEEE Transactions on Plasma Science*, vol. 18, no. 3, pp. 632–645, Jun 1990.

[28] O. A. Nezhevenko, "The magnicon: a new rf power source for accelerators," in *Particle Accelerator Conference, 1991. Accelerator Science and Technology., Conference Record of the 1991 IEEE*, May 1991, pp. 2933–42.

[29] S. H. Gold, C. A. Sullivan, B. Hafizi, and W. M. Manheimer, "Study of gain in c-band deflection cavities for a frequency-doubling magnicon amplifier," *IEEE Transactions on Plasma Science*, vol. 21, no. 4, pp. 383–387, Aug 1993.

[30] O. Nezhevenko, I. Kazarezov, E. Kozyrev, G. Kuznetsov, I. Makarov, A. Nikiforov, B. Persov, G. Serdobintsev, M. Tiunov, V. Yakovlev, and I. Zapryagaev, "First test of the x-band pulsed magnicon," in *Particle Accelerator Conference, 1993., Proceedings of the 1993*, May 1993, pp. 2650–2.

[31] O. A. Nezhevenko, V. P. Yakovlev, S. H. Gold, and B. Hafizi, "Design of a high power x-band magnicon amplifier," *IEEE Transactions on Plasma Science*, vol. 22, no. 5, pp. 785–795, Oct 1994.

[32] Y. Baryshev, I. Kazarezov, E. Kozyrev, G. Kuznetsov, I. Makarov, O. Nezhevenko, B. Persov, M. Tiunov, V. Yakovlev, and I. Zapryagaev, "A 100 mw electron source with extremely high beam area compression," *Nuclear Instruments and Methods in Physics Research Section A: Accelerators, Spectrometers, Detectors and Associated Equipment*, vol. 340, no. 2, pp. 241 – 258, 1994.

[33] R. Harrington, *Time-harmonic electromagnetic fields*, ser. IEEE press series on electromagnetic wave theory. Wiley, 2001.

[34] J. Neilson, S. Tantawi, and V. Dolgashev, "Design of rf feed system and cavities for standing-wave accelerator structure," *Nuclear Instruments and Methods in Physics Research Section A*, vol. 657, no. 1, pp. 52 – 54, 2011.

07 Accelerator Technology

T08 RF Power Sources